NOTE ON SEABED SHEAR STRESS BENEATH BICHROMATIC AND BIDIRECTIONAL WAVES FOR LARGE BED ROUGHNESS

Dag Myrhaug[a]* , Richard R. Simons[b] , Lars Erik Holmedal[a]

[a]Department of Marine Technology

Norwegian University of Science and Technology (NTNU), Trondheim, Norway

[b]Department of Civil, Environmental and Geomatic Engineering, University College London, London, WC1E 6BT, UK

Corresponding author at: Department of Marine Technology, Otto Nielsens vei 10, NO-7491 Trondheim, Norway.

E-mail address: dag.myrhaug@ntnu.no (D. Myrhaug)

Abstract

The seabed shear stress beneath bichromatic and bidirectional waves is presented. The approach is analytical using the constant time-invariant eddy viscosity representation of Christoffersen and Jonsson (1985) for rough turbulent boundary layers under monochromatic waves for large seabed roughness. This formulation is extended to calculate the maximum bed shear stress beneath bichromatic and bidirectional waves by vectorial superposition of the shear stresses for each harmonic wave. Examples of results are given for bichromatic and unidirectional waves as well as bichromatic and bidirectional waves. Comparisons are also made with an equivalent monochromatic wave. The results appear to be in qualitative agreement with physical expectations. Finally, comparison is made with data from small scale laboratory experiments for seabed shear stress beneath bichromatic and unidirectional waves for large bed roughness yielding fair agreement between predictions and data.

1. Introduction

Coastal areas are generally characterized by intermediate and shallow water depths where the kinematics and dynamics of the fluid motion within the seabed boundary layer plays a crucial role governing the flow and sediment transport. The seabed shear stress caused by the boundary layer related friction between the fluid and the seabed affects the sediment transport and morphology, and consequently the stability of scour protections in near-coastal zones. The wave boundary layer has been studied by itself and in combination with the current boundary layer as the flow due to waves interacting with current represents the most common flow condition near the seabed in coastal zones. Generally, real coastal waves are irregular. More details on the background together with reviews of the topic are found in the recent textbook of Sumer and Fuhrman (2020) as well as in the articles by Juan and Dash (2017) and Zhang et al. (2022). More specifically, Yuan and Dash (2017) includes a review of wave boundary layers beneath irregular coastal waves, while Zhang et al. (2022) provides a comprehensive review of wave-current interaction in nearshore areas.

The purpose of this article is to provide the seabed shear stress beneath bichromatic and bidirectional waves using the constant time-invariant eddy viscosity approach of Christoffersen and Jonsson (1985) for rough turbulent boundary layers under sinusoidal waves for large bed roughness. The formulation is extended to calculate the bed friction under bichromatic and bidirectional waves with frequencies ω_1 and ω_2 as well as propagation directions θ_1 and θ_2. The present work, focusing on large bed roughness, is complementary to Myrhaug and Holmedal (1998) providing some aspects of bed friction under bichromatic and bidirectional waves using the two-layer time-invariant eddy viscosity approach of Brevik (1981) valid for small bed roughness. Examples of results for both bichromatic and unidirectional as well as bichromatic and bidirectional waves are given and compared with an equivalent monochromatic wave. The results appear to be in qualitative agreement with physical expectations. Comparisons are also made with data from small scale flume

experiments for the maximum seabed shear stress under bichromatic and unidirectional waves yielding fair agreement between predictions and data.

2. Seabed shear stress beneath bichromatic and bidirectional waves

Two monochromatic waves with wave frequencies ω_1 and ω_2, propagation directions θ_1 and θ_2, and phase angles α_1 and α_2 are considered, with the horizontal free stream wave induced velocity vectors

$$\vec{U}_n = \vec{u}_{0n} e^{i(\omega_n t + \alpha_n)} ; n = 1, 2 \tag{1}$$

and the bed shear stress vectors

$$\vec{\tau}_n = \vec{\tau}_{0n} e^{i(\omega_n t + \hat{\phi}_n)} \quad ; \quad \hat{\phi}_n = \phi_n + \alpha_n ; n = 1, 2 \tag{2}$$

Here $\vec{u}_{0n}$ is the horizontal free stream velocity amplitude vector, $\vec{\tau}_{0n}$ is the bed shear stress amplitude vector, $\hat{\phi}_n$ is the bed shear stress phase, ϕ_n is the phase lag between bed shear stress and velocity, t is the time, and $i = \sqrt{-1}$ is the complex unit. The combined bed shear stress under bichromatic and bidirectional waves is

$$\vec{\tau} = \vec{\tau}_{01} e^{i(\omega_1 t + \hat{\phi}_1)} + \vec{\tau}_{02} e^{i(\omega_2 t + \hat{\phi}_2)} \tag{3}$$

The magnitude of the bed shear stress $\tau = |\vec{\tau}|$ is obtained from Eq. (A4) in Appendix A as

$$\tau^4 = \tau_{01}^4 + \tau_{02}^4 + 4\tau_{01}^2 \tau_{02}^2 \cos^2(\theta_2 - \theta_1) + 4\tau_{01}^2 \tau_{02}^2 \cos^2\left[(\omega_1 - \omega_2)t + \hat{\phi}_1 - \hat{\phi}_2\right]$$

$$-2\tau_{01}^2 \tau_{02}^2 + 4\tau_{01}\tau_{02}(\tau_{01}^2 + \tau_{02}^2)\cos(\theta_2 - \theta_1)\cos\left[(\omega_1 - \omega_2)t + \hat{\phi}_1 - \hat{\phi}_2\right] \tag{4}$$

where $\tau_{0n} = |\vec{\tau}_{0n}|$. For $\omega_1 \neq \omega_2$ the maximum bed shear stress is

$$\tau_{wm} = \left[\tau_{01}^2 + \tau_{02}^2 + 2\tau_{01}\tau_{02}\cos(\theta_1 - \theta_2)\right]^{1/2} \quad ; \omega_1 \neq \omega_2 \tag{5}$$

One should notice that τ_{wm} is independent of the phase angles $\hat{\phi}_1$ and $\hat{\phi}_2$ for $\omega_1 \neq \omega_2$. Except for a special case given in a subsequent example, bichromatic waves (for $\omega_1 \neq \omega_2$) will be considered.

The basis for the present formulation is the Christoffersen and Jonsson (1985) time-invariant eddy viscosity approach for rough turbulent boundary layers under monochromatic waves, i.e., their model 1 for "large roughness", which is valid for fully rough turbulent flow.

According to their formulation the bed shear stress amplitude associated with a sinusoidal wave with wave frequency ω and free stream velocity amplitude u_0 is obtained from the well-known laminar solution given by $\tau_{wm}/\rho = \sqrt{\omega \nu} u_0$ (see e.g. Jonsson (1980, pp.113-115)). The kinematic viscosity ν is replaced by the constant (in time and space) eddy viscosity

$$\varepsilon_w = \beta k_s u_{*wm} \quad ; \quad \beta = 0.0747 \tag{6}$$

where k_s is the Nikuradse equivalent sand roughness, u_{*wm} is the maximum bed friction velocity defined by

$$u_{*wm} = \sqrt{\frac{\tau_{wm}}{\rho}} \tag{7}$$

and ρ is the fluid density. Thus, for a sinusoidal wave the use of Eqs. (6) and (7) yields $u_{*wm}^2 = \tau_{wm}/\rho = \sqrt{\omega \varepsilon_w} u_0 = \sqrt{\beta \omega k_s u_{*wm}} u_0$, and consequently

$$u_{*wm} = (\beta \omega k_s u_0^2)^{1/3} \tag{8}$$

Similarly, using Eqs. (6) and (7) the bed shear stress amplitude associated with each harmonic wave component is

$$\frac{\tau_{0n}}{\rho} = \sqrt{\beta \omega_n k_s u_{*wm}} u_{0n} \tag{9}$$

Combination of Eqs. (5) and (7) yields

$$u_{*wm} = \left[\left(\frac{\tau_{01}}{\rho} \right)^2 + \left(\frac{\tau_{02}}{\rho} \right)^2 + 2 \frac{\tau_{01}}{\rho} \frac{\tau_{02}}{\rho} \cos(\theta_2 - \theta_1) \right]^{1/4} \quad ; \quad \omega_1 \neq \omega_2 \tag{10}$$

Thus, combination of Eqs. (9) and (10) gives the maximum friction velocity as

$$u_{*wm} = \left[u_{01}^2 \omega_1 + u_{02}^2 \omega_2 + 2u_{01}u_{02}\sqrt{\omega_1 \omega_2} \cos(\theta_2 - \theta_1) \right]^{1/3} (\beta k_s)^{1/3} \ ; \ \omega_1 \neq \omega_2 \qquad (11)$$

This approach is valid for $1.3 < a_0 / k_s < 50$ where $a_0 = u_0 / \omega$ is the free stream excursion amplitude (Christoffersen and Jonsson, 1985).

One should note that the friction velocity u_{*wm} associated with the maximum bed shear stress considered here is a relevant physical quantity, e.g. since it is the maximum bed shear stress which is responsible for picking up sediments under waves over a sandy seabed.

3. Results and discussion

This section includes examples of results for bichromatic and unidirectional waves (Section 3.1) as well as bichromatic and bidirectional waves including comparison with an equivalent monochromatic wave (Section 3.2). The examples represent realistic flow conditions in the validity range of the model. Comparisons between predictions and data from direct measurements of bed shear stresses beneath bichromatic and unidirectional waves are also provided (Section 3.3).

3.1 Example 1: Bed shear stress beneath bichromatic and unidirectional waves

For this case Eq. (11) reduces to

$$u_{*wm} = \left[(u_{01}\sqrt{\omega_1} + u_{02}\sqrt{\omega_2})\sqrt{\beta k_s} \right]^{2/3} \ ; \ \omega_1 \neq \omega_2 \qquad (12)$$

where the physical conditions are given in Table 1.

Now the maximum bed shear stress under bichromatic and unidirectional waves will be compared with that obtained by calculating the shear stress separately for each harmonic wave component, and then adding them together (i.e., linear superposition). By using the values in Table 1 with (T, u_0, a_0 / k_s) = (7.2 s, 1.53 m/s, 28) and (6.0 s, 1.53 m/s, 23), respectively, linear superposition gives a value which is 80% of the value obtained by using Eq. (12) given in Table 1. This result is expected because the maximum bed shear stress is

proportional to the velocity squared, i.e., $\tau_{wm} = 0.5\rho u_0^2 f_w$ where f_w is the wave friction factor. Thus, $\tau_{wm}/\rho \sim (u_0 + u_0)^2 = 4u_0^2$, while linear superposition gives

$\tau_{wm}/\rho \sim u_0^2 + u_0^2 = 2u_0^2$, which is smaller than the other value, suggesting smaller values by linear superposition. One should notice that this example value (80%) is not a general rule, which is demonstrated in Section 3.3.

Comparison with an equivalent monochromatic wave

The wave induced velocity near the seabed under the two waves considered in this example is

$$u = u_0 \cos \omega_1 t + u_0 \cos \omega_2 t = 2u_0 \cos(\Delta\omega t)\cos\bar{\omega}t \tag{13}$$

where $\Delta\omega = (\omega_2 - \omega_1)/2 = 0.08725$ rad/s and $\bar{\omega} = (\omega_1 + \omega_2)/2 = 0.9595$ rad/s. The equivalent monochromatic wave considered here is $u = U_0 \cos\bar{\omega}t$. By using Eqs. (7) and (8) replacing u_0 in Eq. (8) with $2u_0 = 3.06$ m/s and $\omega = \bar{\omega} = 0.9595$ rad/s, it is found that $\tau_{wm}/\rho = 0.1214$ m²/s², which is close to that for bichromatic waves in Example 1, i.e. $\tau_{wm}/\rho = 0.1212$ m²/s² by including four decimals. One should notice that a first approximation to long-crested irregular waves is obtained by taking $\Delta\omega \ll 1$ in Eq. (13) (see e.g. Crapper (1984)).

3.2 Example 2: Bed shear stress beneath bichromatic and bidirectional waves

As an example the friction velocity is determined from Eq. (11) with $\theta_2 - \theta_1 = 45^o$ and the conditions given in Table 1. The result is given in Table 1, showing that the maximum bed shear stress is smaller under bidirectional waves than under unidirectional waves, as expected.

Furthermore, linear superposition of the two resulting shear stress amplitudes for regular waves using Eq. (5) (i.e. $\tau_{wm}/\rho = 0.0891 m^2/s^2$), yields a value which is 82% of the solution obtained using Eq. (11) given in Table 1. It should be noted that Eq. (5) is the general solution which is used to linearly superpose the two shear stress amplitudes in Table 1. Furthermore, by combining Eq. (5) with Eqs. (6), (7), (9) and (10) this yields Eq. (11) representing the result of the interaction between the two shear stress components. As in Example 1 this result is expected but is not a general value. Now

6

$\tau_{wm}/\rho \sim u_0^2 + u_0^2 + 2u_0u_0 \cos 45° = 2u_0^2(1 + \cos 45°)$. Linear superposition gives

$\tau_{wm}/\rho \sim (u_0^4 + u_0^4 + 2u_0^2u_0^2 \cos 45°)^{1/2} = \sqrt{2}u_0^2(1 + \cos 45°)^{1/2}$, which is smaller than the other value, suggesting smaller values by linear superposition.

Comparison with an equivalent monochromatic wave

To make comparison with an equivalent monochromatic wave, this example is simplified by considering

Wave 1: $T = 7.2s, u_0 = 1.53\text{m/s}, \alpha_1 = 0, \theta_1 = 0$ (14)

Wave 2: $T = 7.2s, u_0 = 1.53\text{m/s}, \alpha_2 = 0, \theta_2 = 45°$ (15)

Then, the horizontal wave induced velocity near the seabed under these two waves is

$$u = u_0 \cos(kx - \omega t) + u_0 \cos(kx\cos\theta_2 + ky\sin\theta_2 - \omega t)$$

(16)

$$= 2u_0 \cos\frac{1}{2}[kx(1 - \cos\theta_2) - ky\sin\theta_2]\cos\left\{\frac{1}{2}[kx(1 + \cos\theta_2) + ky\sin\theta_2] - \omega t\right\}$$

where x and y are horizontal coordinates, and k is the wave number determined from the dispersion relationship $\omega^2 = gk\tanh kh, h$ is the water depth, and g is the acceleration due to gravity. The second cosine-term is the mean wave with frequency ω and wave number vector $\vec{k} = k(1 + \cos\theta_2, \sin\theta_2)$. Thus, this wave propagates in the positive $x-$ and $y-$direction with the angle $\theta_2/2$ relative to the x-axis, since $\tan(\theta_2/2) = \sin\theta_2/(1 + \cos\theta_2)$. Moreover, $2u_0$ times the first cosine-term represents a variable amplitude with the "wave number" $\vec{l} = k(1 - \cos\theta_2, -\sin\theta_2)$, and is at a right angle to the second cosine-term since $\vec{k}\cdot\vec{l} = 0$. One should notice that a first approximation to short-crested irregular waves is obtained by taking $\theta_2 \ll 1$ in Eq. (16) (see e.g. Crapper (1984)). Although $\omega_1 = \omega_2$ in this case, Eqs. (10) and (11) are valid since $\hat{\phi}_1 = \hat{\phi}_2$ (see Eq. (4)).

The solution of Eq. (11) with Eqs. (14) and (15) as input is

$$u_{*wm} = 0.320\frac{m}{s} \; ; \; \frac{\tau_{wm}}{\rho} = 0.103\frac{m^2}{s^2}$$

(17)

The equivalent monochromatic wave considered is here taken as $u = 2u_0 \cos(\theta_2 / 2) \cos \omega t$ based on the physical interpretation of Eq. (16) as discussed above. By using Eqs. (7) and (8) replacing u_0 in Eq. (8) with $2u_0 \cos(\theta_2 / 2) = 3.06 \cos 22.5^o = 2.827$ m/s and $\omega = 0.8722$ rad/s, it is found that $u_{*wm} = 0.320$ m/s, $\tau_{wm}/\rho = 0.103$ m²/s², which is identical to the result in Eq. (17). This is expected since Eq. (11) reduces to that for the equivalent monochromatic wave in this case.

One should notice that although the results in Examples 1 and 2 agree qualitatively with physical expectations as well as with the results in Myrhaug and Holmedal (1998), the adequacy of the model can only be verified against relevant data.

3.3 Comparison with measurements

The present data are from laboratory measurements of bed shear stresses under regular as well as bichromatic and unidirectional waves for low orbital excursion amplitude to roughness ratios (a_0 / k_s). The description of the measurement technique is given in Simons and MacIver (2001), while the present data are unpublished data from the same KADWCI project referred to in the Acknowledgements. The tests were carried out in a wave-current flume with water depth $h = 0.40$ m. The bed shear stresses were measured directly at a fixed rough bed by using a shear plate device (Grass et al., 1995) together with simultaneous measurements of flow kinematics. The shear stresses and velocities were measured synchronously and were subject to post-processing to remove the edge pressure effect on the shear stress plate. The two-dimensional bed roughness consisted of roughness elements of 6 mm square cross-sections, placed at 25 mm centers across the line of flow, with an observed Nikuradse sand roughness $k_s = 36$ mm. For all tests the bed shear stress has been obtained by correcting the total measured force by subtracting the pressure force caused by pressure gradients acting on the shear cell as well as on the vertical faces of individual roughness elements.

The actual test conditions for the data used here are given in Table 2, together with some results which will be discussed in the forthcoming. It appears that the data are outside the validity range of the model, i.e. $a_0 / k_s < 1.3$ (see Table 2). It is noted that the Reynolds numbers are also rather low with $Re = u_0 a_0 / v = 4 \cdot 10^2 - 3 \cdot 10^3$. Thus, the data are not in the

fully rough turbulent flow regime since $\mathrm{Re} < 10^4$ (e.g. see Fig. 3 in O´Donoghue et al. (2021)). However, despite of this and due to lack of other data, these data will be used for comparison with predictions, which are valid for fully rough turbulent flow.

First, the harmonic wave results W1, W2 and W3 for the flow conditions in terms of T, u_0, a_0 / k_s and the measured shear stress τ_{wm} are given in Table 2. It appears that the data corresponding to the three harmonic wave conditions are well predicted with the predicted to measured ratios of the maximum bed shear stress in the range 0.95 to 1.06. It should be noted that use of the Simons et al. (2000) friction factor formula, i.e.

$$f_w = 0.33(\frac{a_0}{k_s})^{-0.84} \ ; \ \frac{a_0}{k_s} < 30 \tag{18}$$

yields $\tau_{wm} = (0.99, 1.46, 1.90) \, N/m^2$ for W1, W2, W3, respectively, showing good agreement with the present predictions and the data. This friction factor was obtained as a best fit to data from a wide range of experiments (flume, oscillating water tunnel).

Second, sequences of the time series for the bichromatic wave results W1&W2 and W1&W3 are depicted in Figs. 1 and 2, respectively, showing τ versus t in Figs. 1a and 2a, while Figs. 1b and 2b show u versus t. It appears that the results in Fig. 1 exhibit the features of a narrow-band process while those in Fig. 2 are more broad-banded. This is as expected due to the smaller difference between wave periods for W1&W2 than for W1&W3.

The predicted values of τ_{wm} for W1&W2 and W1&W3 are based on using the flow conditions for W1, W2 and W3 from Table 2 as input in Eq. (12). From Table 2 it appears that $\tau_{wm} = 3.0 \, N/m^2$ for both conditions, while the predicted to measured ratios of τ_{wm} is 0.91 for W1&W2 and 1.15 for W1&W3. Furthermore, the predictions of the bichromatic waves also exhibit the expected features demonstrated in Example 1, i.e. linear superposition of the values for each harmonic wave gives a value which is smaller than the bichromatic values. The result for W1&W2 shows this (i.e. $\tau_{wm} = (0.88 + 1.36)N/m^2 = 2.24N/m^2 < 3.0N/m^2$). This is also the case for W1&W3 although the difference is smaller than for W1&W2 (i.e. $\tau_{wm} = (0.88 + 1.83) \, N/m^2 = 2.71 \, N/m^2 < 3.0 \, N/m^2$). However, it should be noted that the predicted value of τ_{wm} for W1&W2 is smaller than for W1&W3 while the measured values are

the same. The reason for this is not clear for the authors, although the fact that the measurements are not in the fully rough turbulent flow regime might play a role.

Knowledge of the results in Figs. 1 and 2 can also be used to estimate τ_{wm} based on the maximum wave induced velocity obtained from the figures. That is, the values of T, u_0 and a_0 / k_s in Table 2 for W1&W2 and W1&W3 correspond to the wave with the largest maximum wave induced velocity. Use of the Simons al. (2000) formula in Eq. (18) yields $\tau_{wm} = (2.47, 2.87) N / m^2$ for W1&W2 and W1&W3, respectively. Alternatively, Eqs. (7) and (8) can be used to estimate τ_{wm}, i.e. $\tau_{wm} = \rho u_0^{4/3} (\beta k_s 2\pi / T)^{2/3}$. With the values in Table 2 this yields $\tau_{wm} = (2.44, 2.97) N / m^2$ for W1&W2 and W1&W3, respectively, which agrees well with those using the Simons et al. formula. One should notice that these estimates are not predictions since they are based on using the observed results as input.

However, comparison with data in the validity range of the model is required to make firm conclusions regarding the validity of the method.

4. Conclusions

An extension of the Christoffersen and Jonsson (1985) model for predicting seabed shear stresses beneath bichromatic and bidirectional waves valid for $1.3 < a_0 / k_s < 50$ in the fully rough turbulent flow regime is provided. The main conclusions are:

1. The approach appears to give results in qualitative agreement with physical expectations.

   Examples of results show that:

   a) The maximum bed shear stress under bichromatic and unidirectional waves as well as well as under bichromatic and bidirectional waves are larger than the values obtained by linear superposition of the values for each monochromatic wave.

   b) The maximum bed shear stress under bichromatic and bidirectional waves is smaller than under bichromatic and unidirectional waves.

   c) The maximum bed shear stress under bichromatic/bidirectional waves is close/identical to the maximum bed shear stress under a monochromatic wave

with velocity amplitude equal to the maximum velocity of the bichromatic/bidirectional wave and with wave frequency equal to the mean of the two frequencies of the bichromatic wave/wave direction equal to the mean direction of the bidirectional wave.

2.   The model predictions valid for fully rough turbulent flow are compared with data from measurement of the maximum bed shear stress from small scale laboratory experiments, although the data are not in the fully rough turbulent flow regime with $a_0/k_s < 1.3$ and $Re < 10^4$.

a) The data corresponding to the three harmonic wave conditions are well predicted with the predicted to measured ratios of the maximum bed shear stress in the range 0.95 to 1.06.

 b) Overall, the present approach gives an adequate representation of the data for the maximum bed shear stress under bichromatic and unidirectional waves. The data associated with the two bichromatic wave records show that linear superposition of the values for each monochromatic wave gives values which are smaller than the bichromatic values.

3.   Comparison with data in the validity range of the model is required to make firm conclusions regarding the validity of the method.

Appendix A

By introducing $\gamma_n = \omega_n t + \hat{\phi}_n$ for $n = 1, 2$ in Eq. (3):

$$\vec{\tau} = \vec{\tau}_{01} e^{i\gamma_1} + \vec{\tau}_{02} e^{i\gamma_2} \tag{A1}$$

Then, by using Eq. (A1) the magnitude of the bed shear stress vector, $|\vec{\tau}|$, is obtained as

$$|\vec{\tau}|^2 = \vec{\tau} \cdot \vec{\tau} = \tau_{01}^2 e^{i2\gamma_1} + \tau_{02}^2 e^{i2\gamma_2} + 2\tau_{01}\tau_{02} \cos(\theta_2 - \theta_1) e^{i(\gamma_1 + \gamma_2)} \tag{A2}$$

where $\tau_{0n} = |\vec{\tau}_{0n}|$. Thus, the magnitude of the bed shear stress, τ, is obtained as the magnitude of the complex quantity in Eq. (A2) as (by denoting A^* as the complex conjugate of A)

$$\tau^4 = |\vec{\tau}|^2 \, (|\vec{\tau}|^2)^*$$

$$= [\tau_{01}^2 e^{i2\gamma_1} + \tau_{02}^2 e^{i2\gamma_2} + 2\tau_{01}\tau_{02} \cos(\theta_2 - \theta_1) e^{i(\gamma_1 + \gamma_2)}][\tau_{01}^2 e^{-i2\gamma_1} + \tau_{02}^2 e^{-i2\gamma_2} + 2\tau_{01}\tau_{02} \cos(\theta_2 - \theta_1) e^{-i(\gamma_1 + \gamma_2)}]$$

$$\tag{A3}$$

Then, Eq. (4) follows by using the relationships $\cos x = (e^{ix} + e^{-ix})/2$, $\cos 2x = 2\cos^2 x - 1$, and substituting $\gamma_n = \omega_n t + \hat{\phi}_n$ for $n = 1, 2$:

$$\tau^4 = \tau_{01}^4 + \tau_{02}^4 + 4\tau_{01}^2 \tau_{02}^2 \cos^2(\theta_2 - \theta_1) + 4\tau_{01}^2 \tau_{02}^2 \cos^2(\gamma_1 - \gamma_2)$$

$$\tag{A4}$$

$$-2\tau_{01}^2 \tau_{02}^2 + 4\tau_{01}\tau_{02}(\tau_{01}^2 + \tau_{02}^2)\cos(\theta_2 - \theta_1)\cos(\gamma_1 - \gamma_2)$$

References

Brevik, I. (1981). Oscillatory rough turbulent boundary layers. J. Waterways, Port, Coastal and Ocean Eng., ASCE, 107(3): 175-188.

Christoffersen, J.B. and Jonsson, I.G. (1985). Bed friction and dissipation in a combined current and wave motion. Ocean Engng., 12(5): 387-423.

Crapper, G.D. (1984). Introduction to water waves. Ellis Horwood Ltd. Chichester, UK.

Grass, A.J., Simons, R.R., MacIver, R.D., Mansour-Tehrani, M. and Kalopedis, A. (1995). Shear cell for direct measurements of fluctuating bed shear stress vector in combined wave/current flow. Proc. XXVIth IAHR Congress: Hydraulic Research and its

Jonsson, I.G. (1980). A new approach to oscillatory rough turbulent boundary layers. Ocean Engng., 7(1): 109-152.

Myrhaug, D. and Holmedal, L.E. (1998). Aspects of seabed shear stresses under long-crested and short-crested irregular waves. Proc. 3rd Int. Conf. on Hydroscience and Engineering, Cottbus, Germany.

O´Donoghue, T., Davies, A.G., Bhawanin, M. and van der A, D.A. (2021). Measurement and prediction of bottom boundary layer hydrodynamics under modulated oscillatory flows. Coastal Eng., 169: 103954.

Simons, R.R. and MacIver, R.D. (2001). Regular, bichromatic and random waves on co-linear currents. Proc. 4th Conf. on Coastal Dynamics, ASCE, Lund, Sweden, Vol.1, pp. 216-226.

Simons, R.R., Myrhaug, D., Thais, L., Chapalain, G., Holmedal, L.E. and MacIver, R.D. (2000). Bed friction in combined wave-current flows. Proc. 27th Int. Conf. on Coastal Eng., ASCE, Sydney, Australia, pp. 216-226.

Sumer, B.M. and Fuhrman, D.R. (2020). Turbulence in Coastal and Civil Engineering. World Scientific, Singapore.

Yuan, J. and Dash, S.M. (2017). Experimental investigation of turbulent wave boundary layers under irregular coastal waves. Coastal Eng., 128: 22-36.

Zhang, X., Simons, R., Zheng, J. and Zhang, C. (2022). A review of the state of research on wave-current interaction in nearshore areas. Ocean Eng., 243: 110202.

Table 1. Example of results; $k_s = 0.063\,\text{m}$.

Example	Wave condition	T (s)	u_0 (m/s)	$\dfrac{a_0}{k_s}$	τ_{wm}/ρ (m²/s²)
	Regular (W1)	7.2	1.53	28	0.0453
	Regular (W2)	6.0	1.53	23	0.0511
1	Bichromatic (W1&W2) & unidirectional ($\Delta\theta = 0\,°$)				0.121
2	Bichromatic (W1&W2) & bidirectional ($\Delta\theta = 45°$)				0.109

Table 2.   Comparison between data and predictions: k_s = 0.036 m.

Main flow variables and measured results						Predicted
Record	Wave condition	T (s)	u_0 (m/s)	$\dfrac{a_0}{k_s}$	τ_{wm} (N/m²)	τ_{wm} (N/m²)
280598 m.duc	regular (W1)	1.333	0.044	0.26	0.88	0.84
280598 ac.duc	regular (W2)	1.422	0.064	0.40	1.36	1.33
289598 s.duc	regular (W3)	1.778	0.095	0.75	1.83	1.94
280598 g.duc	bichromatic (W1&W2)[*]	1.4	0.10	0.62	3.0	2.72
040698 m.duc	bichromatic (W1&W3)[*]	1.5	0.12	0.80	3.0	3.44

[*]For these conditions the values of *T*, u_0 and a_0/k_s correspond to the wave with the largest maximum wave induced velocity obtained from Figs. 1b and 2b.

Figure captions

Figure 1. Sequences of time series for the bichromatic wave results W1&W2: (a) the shear stress τ versus t; (b) the horizontal free stream wave induced velocity u versus t.

Figure 2. Sequences of time series for the bichromatic wave results W1&W3: (a) the shear stress τ versus t; (b) the horizontal free stream wave induced velocity u versus t.
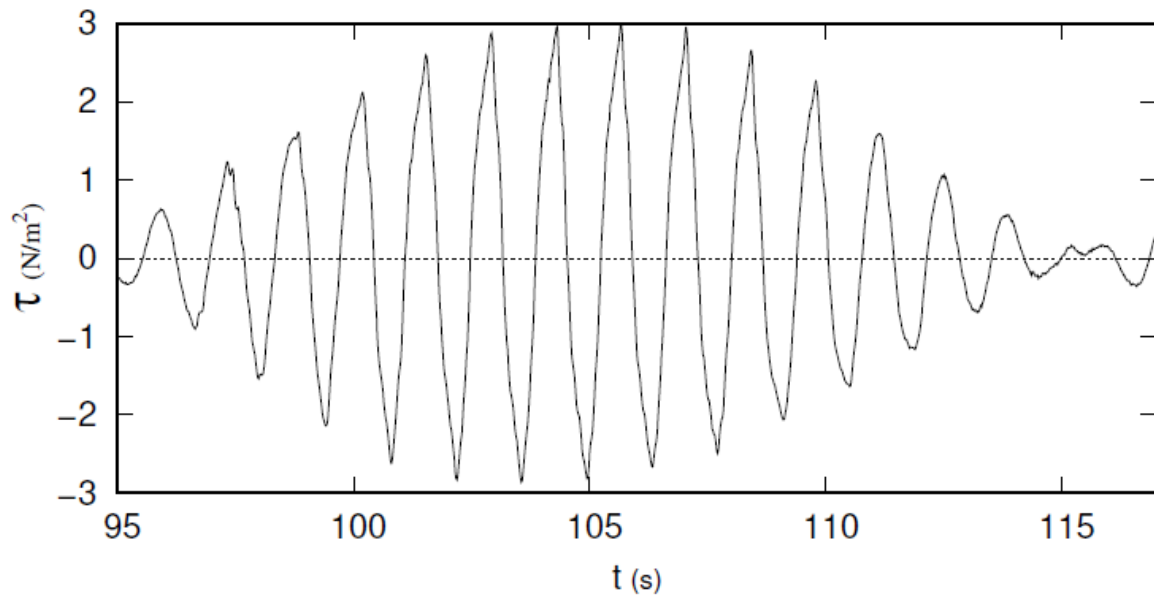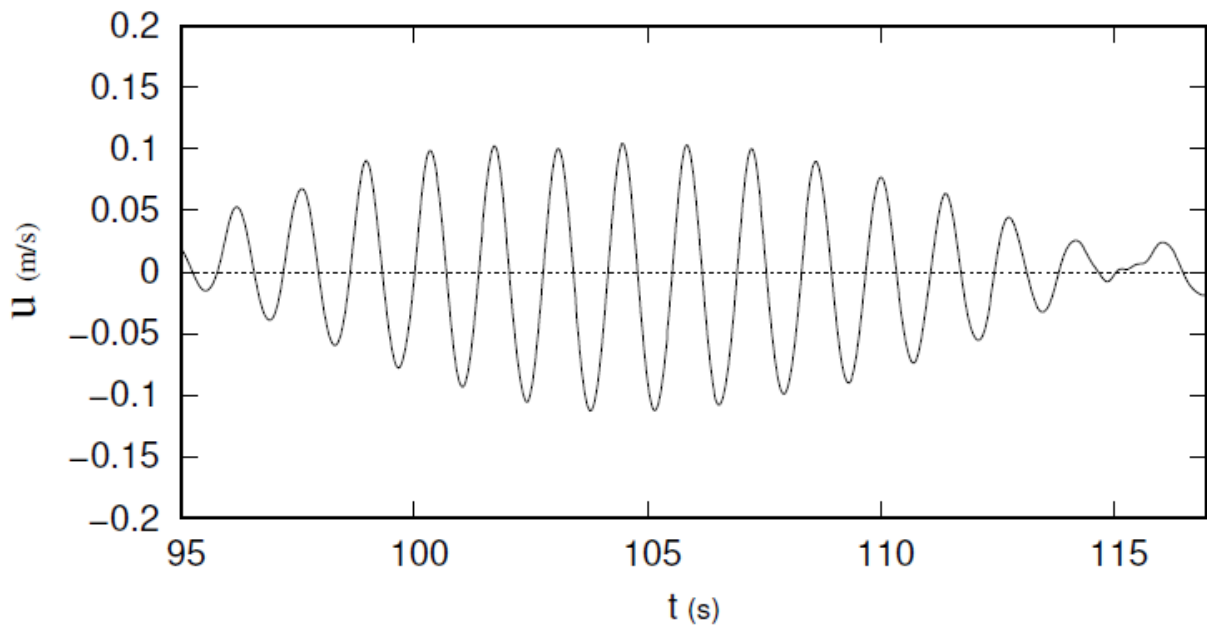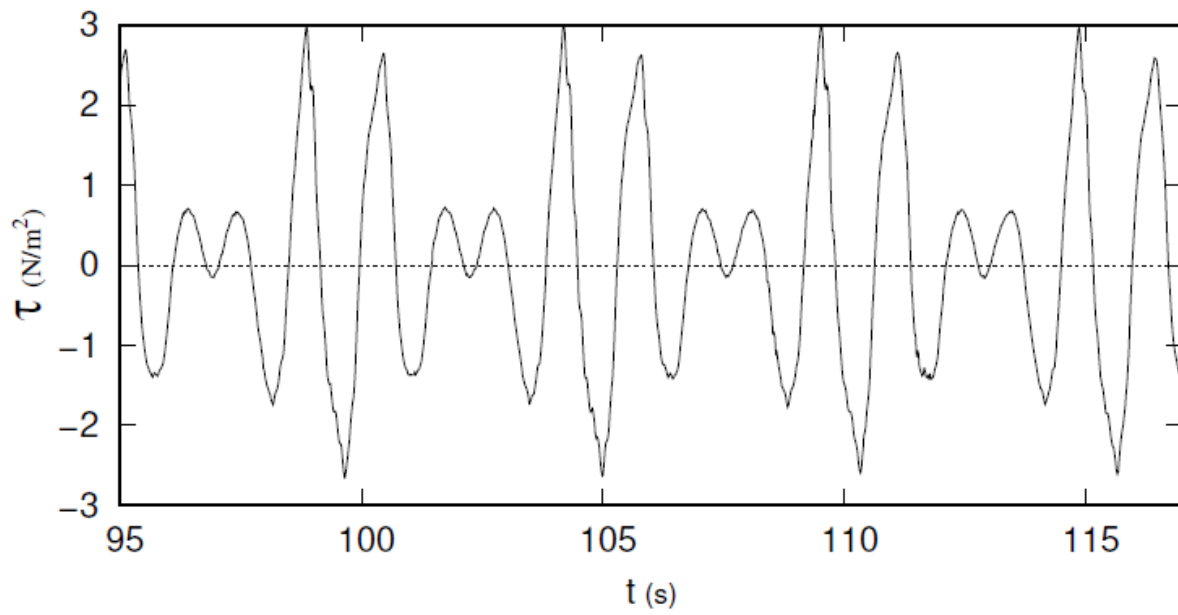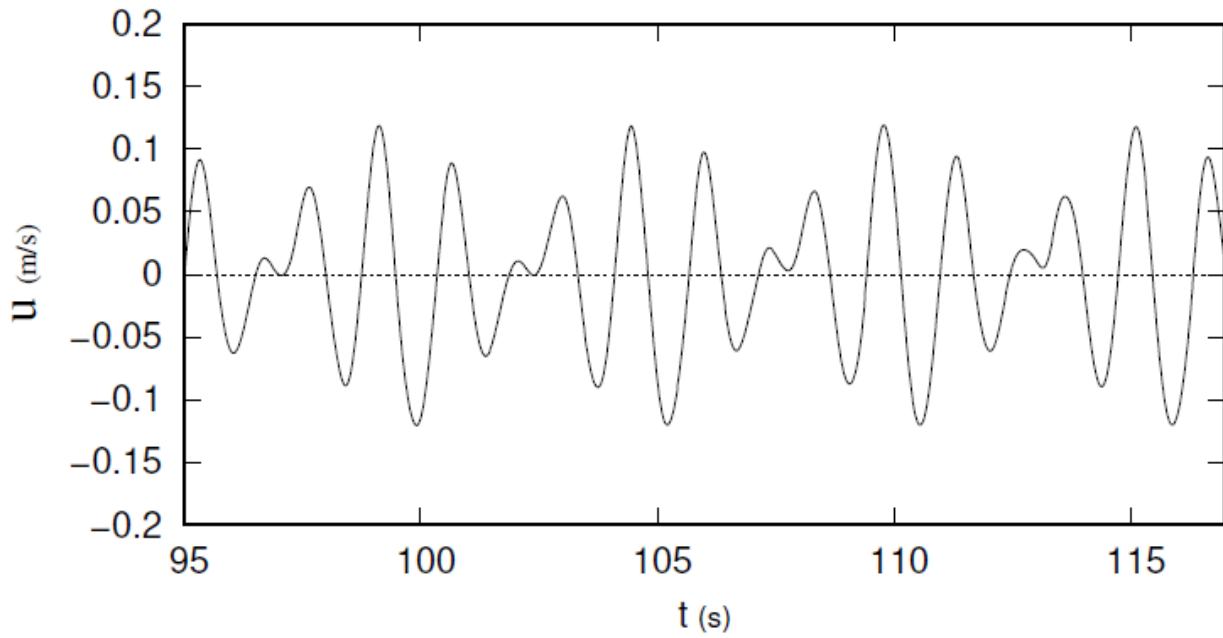
Fig. 1(a)

Fig. 1(b)

17

Fig. 2(a)

Fig. 2(b)